Mitigation of Rain and Ice Particle Cross Polarization at RF for Dual Circularly Polarized Waves

Kiyo Tomiyasu, *Life Fellow, IEEE*

***Abstract*—On millimeter-wave satellite-to-ground links encountering moderate rain and ice particles, RF mitigation of atmospheric cross-polarization effects on circularly polarized (CP) waves can be achieved by inserting a passive fixed phase delay in the vertical component of the received electric field introduced prior to an orthomode transducer (OMT) in the receiver. This passive phase shifter and the OMT can be combined into a single microwave structure and its performance is discussed.**

***Index Terms*— Circularly polarized waves, ice depolarization, millimeter waves, mitigation technique, rain depolarization.**

I. Introduction

TO MEET the ever-increasing bandwidth needs on satellite-to-ground communication links, frequency reuse systems can be designed utilizing orthogonal polarizations for two channels. Orthogonal linear polarizations are used on the TDRSS up and down links at S and K_u bands [1]. An impairment on dual-orthogonal circularly polarized (CP) channels is the amount of cross polarization or interference caused by nonspherical rain and ice particles along the link [2]. Since the amount of cross polarization is related to atmospheric phenomena, it is a random parameter that increases the difficulty in its mitigation or cancellation. In this paper, a passive fixed phase delay added at RF is suggested, capable of mitigating a significant amount of cross polarization caused by moderate rain and ice particles on a satellite-to-ground link operating in the 20-GHz and higher frequency region.

For space-to-ground links, the use of CP instead of linearly polarized waves offers the advantage of freedom of geometric orientation of the transmitting and receiving antennas. However, the mount of cross polarization caused by rain and ice particles depends on the polarization state and it is greater on a circularly polarized link than on either a vertical or horizontal linearly polarized link. There is a preponderance of evidence that during rain, ice particles are simultaneously present in the upper atmosphere that affect link performance at the higher frequencies. Arnold *et al.* [3] reported that the major axes of rain and ice particles are nearly horizontal. Other investigators have also reported this orientation [4]–[12]. One group using a multiparameter radar reported on the existence of vertically oriented ice crystals [13]; this existence will help mitigate the depolarization due predominately to horizontally oriented crystals [2], [3], [7], [8], [11].

Manuscript received December 5, 1996; revised February 23, 1998.

The author is with the Lockheed Martin Corporation, Philadelphia, PA 19101 USA.

Publisher Item Identifier S 0018-926X(98)06878-1.

This paper discusses: 1) the propagation of polarized waves; 2) the generation of cross polarization and its definition; 3) a simple mitigation circuit design employing a fixed phase shifter (delay) that operates at RF for dual CP signals; and 4) the performance of a proposed microwave component that combines this fixed phase shifter with an orthomode transducer (OMT) into a special transducer. The analysis shows that cross-channel interference on CP signals can be significantly reduced by this simple mitigation circuit and this approach has been reported earlier [5], [7], [8]. The analysis has revealed that the net performance of this RF mitigation technique, in general, is not equal in magnitude between an incident right CP wave and a left CP wave. Equal performance is possible, however, if a modest amount of cross-channel interference is allowed in each of the two channels.

II. Cross-Polarization Mitigation Approaches

Papers have been published describing various methods of reducing the adverse cross-polarizing effects caused by rain [2], [14], [15]. Some methods achieve this objective by modifying the RF portion at the input of the receiver. Complete compensation of the cross polarization at RF or total restoration of wave polarization purity requires adding some loss to the RF restoration circuit. This will degrade the net G/T of the receiver, but this degradation can be mitigated by amplifying the incoming signals prior to the restoration circuit at RF. A cross polarization cancellation method has been described that utilizes dual cross-coupling circuits between the two "orthogonally" polarized output channels [2], [14], [15].

III. Cross-Polarization and Random Polarization

In this section, the issues discussed are: 1) cross-pol discrimination; 2) random polarization; 3) cross polarization of a circularly polarized wave; 4) emerging polarization ellipse; 5) cross-pol discrimination of an elliptically polarized wave; and 6) near-constant ellipse tilt angle.

A. Cross-Pol Discrimination

A term often used to describe link performance degradation due to rain is cross-pol discrimination, which is the coupling or leakage of a signal in a primary (co-pol) channel into a secondary (cross-pol) channel. To portray simply the magnitude of the interference, the term XPD is often used, which is a scalar quantity defined as a power ratio given by Stutzman

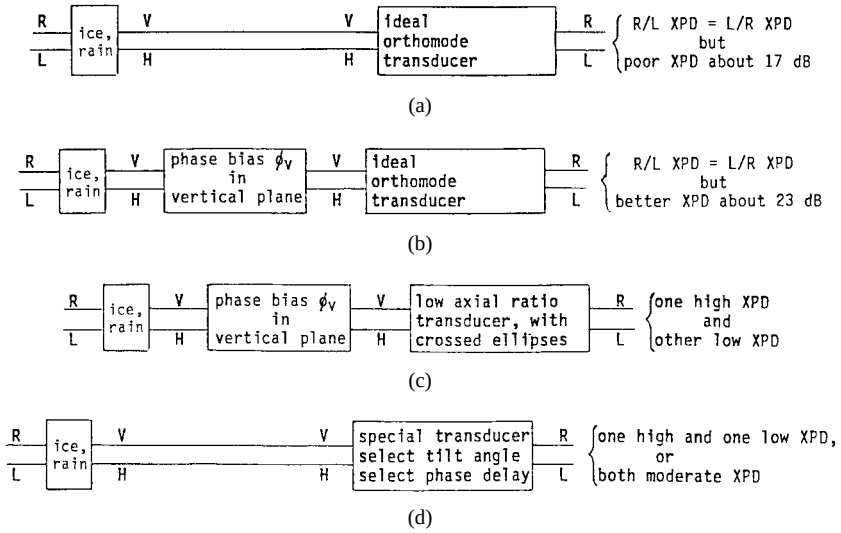

Fig. 1. Rain and ice particle cross-polarization mitigation circuits.

[16]

$$\text{XPD} = \frac{\text{power received in intended channel}}{\text{power received in unintended channel}}. \quad (1)$$

Note that the magnitude of XPD is greater than unity. It should be stated that for a given propagation path anisotropy, XPD will differ, in general, depending on the incoming polarization state, i.e., linearly polarized V/H XPD is not numerically equal to circularly polarized R/L XPD. This is discussed later and in another paper by the author [17].

For system network analysis, however, a scalar XPD is insufficient for treating cascaded networks. For this purpose, the complex value of XPD is essential denoted as $\mathbf{XPD}$, which is the ratio of the complex signals in the intended and unintended channels [17].

B. Random Polarization

Wave depolarization or cross polarization due to rain and ice is time dependent and probably frequency dependent as well. This depolarized wave has some resemblance to radiation from stars and can be described by orthogonally polarized components plus a randomly polarized component. Stellar radiation is characterized by Stokes parameters [18], [19], which are ensemble averages of the two polarized components in both time and frequency. The randomly polarized component is sometimes called unpolarized component [19], but this topic is not addressed here. Its magnitude is not known for a propagation link with rain, but can probably be measured. It is believed that this random polarization component cannot be cancelled nor easily mitigated by elementary approaches.

C. Cross Polarization of a Circularly Polarized Wave

In Fig. 1(a), two CP waves are shown incident on a path with rain and ice particles. Each wave, in general, will emerge from the path elliptically polarized caused by its horizontal (H) component slightly weaker and phase delayed relative to the vertical (V) component due to ice particles and rain with major axes nearly horizontal. The two emerging polarization ellipses will be tilted with respect to the horizontal. If an elliptically polarized wave is coupled to an ideal quarter-wave plate OMT, one output port will receive the dominant signal and the other will receive a smaller signal representing the cross-pol component. The opposite CP incident wave will also emerge from the rain and ice particles as an elliptically polarized wave with the same axial ratio, but with the polarization ellipse tilted in the opposite direction with respect to the horizontal by the same amount [20]. The relative magnitudes of the two cross-pol signals will be identical, but the phases may not be [17]. In the next section, elliptical polarization is described and followed by cross-pol discrimination.

D. Emerging Polarization Ellipse

Each emerging elliptically polarized wave can be described by a semi-major axis (OA), a semi-minor axis (OB), and an ellipse tilt angle. A generalized formulation entailing the vertical and horizontal components and an ellipse tilt angle is given by Born and Wolf [19]. For the present analysis, another formulation given by Balanis [21], [22] has been found more convenient since all ellipse parameters can be derived directly from the complex vertical and horizontal components as

$$\begin{aligned} OA &= [0.5(E_v^2 + E_h^2 + K^{0.5})]^{0.5} \\ OB &= [0.5(E_v^2 + E_h^2 - K^{0.5})]^{0.5} \end{aligned} \quad (2)$$

where

E_v	amplitude of vertical electric field;
E_h	amplitude of horizontal electric field;
K	$E_v^4 + E_h^4 + 2E_v^2E_h^2\cos(2\phi_{vh})$;
ϕ_{vh}	$\phi_v - \phi_h$;
ϕ_v	phase of E_v;
ϕ_h	phase of E_h.

The axial ratio (AR) is by definition

$$\text{AR} = OA/OB$$

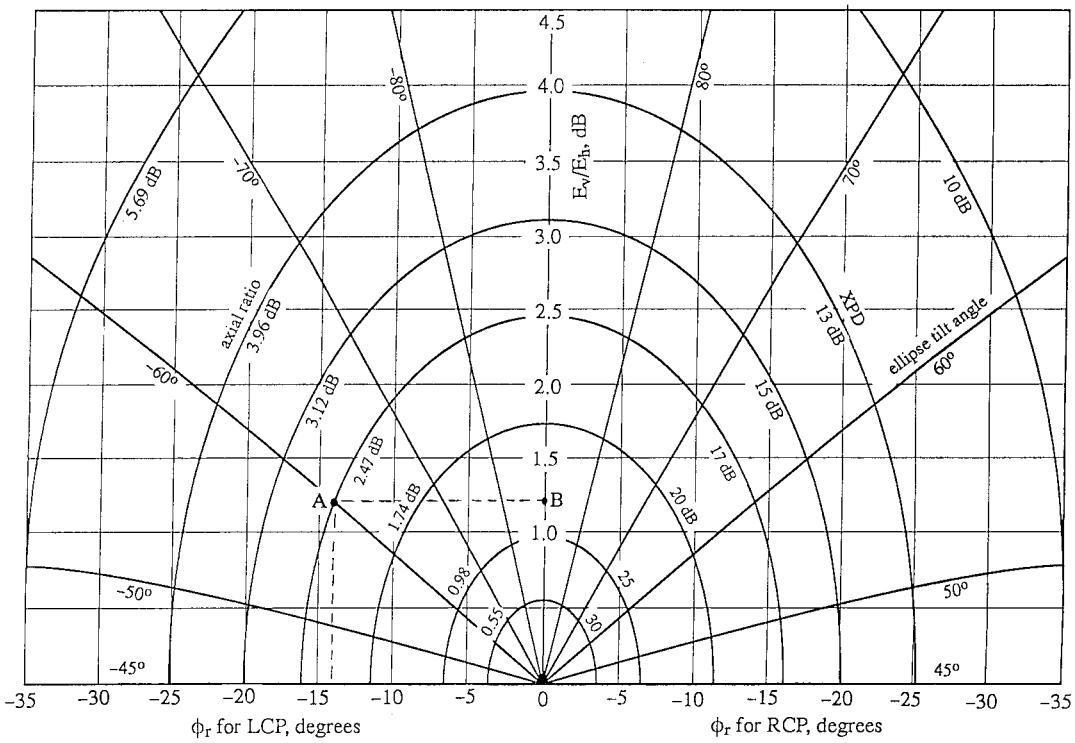

Fig. 2. Cross polarization of an incident circularly polarized wave caused by atmospheric anisotropy. The left side is for a left-hand elliptically polarized wave. The right side is for a right-hand elliptically polarized wave. The ordinate is the amplitude ratio E_v/E_h in decibels. The abscissa is the phase delay differential ϕ_r of the horizontal component relative to that of the vertical component of the emerging wave caused by rain and ice. The ellipse tilt angle is referred to the horizontal. As an illustrative example, initial differentials are 14° and 1.2 dB and the XPD is 17 dB, as shown by point "A." By cancelling the phase difference of 14°, the XPD can be improved to 23 dB as indicated by point "B."

Cross-pol discrimination discussed later is related to AR by the following:

$$\text{XPD} = 20\log_{10}\frac{\text{AR}+1}{\text{AR}-1}. \tag{3}$$

The ellipse tilt angle θ_t relative to the horizontal plane is given in Balanis [21] as

$$\theta_t = 90 - 0.5\tan^{-1}[(2\cos\phi_{\text{vh}})/(\text{E}_\text{h}/\text{E}_\text{v} - \text{E}_\text{v}/\text{E}_\text{h})]. \tag{4}$$

The arctangent is computed in degrees. This formulation avoids the polarization state double-angle ambiguity encountered with the Poincare sphere equations. It is noted in (4) that if $\phi_{vh} = 90°$, the tilt angle θ_t is always $90°$ from the horizontal that is vertical and is independent of the ratio E_v/E_h except if $E_v = E_h$ a tilt angle cannot be defined. The emerging polarization ellipse axial ratio, tilt angle, and XPD are plotted in Fig. 2 for an incident circularly polarized wave. The ordinate is the ratio of E_v/E_h in decibels and the abscissa is ϕ_r, which is the additional phase shift due to rain between the horizontal component relative to the vertical. This type of plot has been published earlier [23].

E. Cross-Pol Discrimination of an Elliptically Polarized Wave

A generalized formulation for cross polarization of a four-port network [17] is applied to the configuration shown in Fig. 1(a). For one example, a right-hand CP wave whose horizontal component is phase delayed by 90° relative to the vertical, is incident on a medium containing rain. A path containing ice is discussed later. Due to the rain, the emerging E_h component is weaker in amplitude than the E_v component and the E_h phase is further delayed by ϕ_r due to the rain. This wave is referred to as the right-hand elliptically polarized (RHEP). This RHEP signal emerging from the rain is incident on an OMT such as a quarter-wave dielectric plate ($\phi_d = 90°$), inclined at an angle $\theta_d = 45°$ relative to vertical [17]. The cross-polarized wave output from the OMT will appear at the two orthogonally polarized ports representing the right (R) and left (L) hand CP components. The power ratio of these two components, a scalar, is called cross-pol discrimination (XPD) [16], [17], as discussed above, and is derived in the Appendix.

Using the derivations in the Appendix, the magnitude of XPD for the elliptically polarized wave emerging from the rain medium in terms of E_v and E_h components of the emerging wave for an incident CP wave is

$$\text{XPD}_{\text{RHEP}} = 20\log_{10}\left|\frac{\text{E}_\text{v} + \text{E}_\text{h}\text{e}^{\text{j}\phi_\text{r}}}{\text{E}_\text{v} - \text{E}_\text{h}\text{e}^{\text{j}\phi_\text{r}}}\right|. \tag{5}$$

For example, if the phase and amplitude differences are 14° and 1.2 dB, respectively, the amplitude of XPD is 17.03 dB, the axial ratio is 2.46 dB, and the ellipse tilt angle is about 60°. This function is also plotted in Fig. 2.

It is noted that while the magnitude of XPD for an incident RCP wave is equal in magnitude to the XPD for an incident LCP wave, the phase of these two complex XPD values are not necessarily equal [17].

F. Near Constant Ellipse Tilt Angle

For an ideal incident CP wave, the ϕ_v differs from ϕ_h by 90°, but with rain or ice particles there is an additional phase shift (delay) of ϕ_r and an additional attenuation on the horizontal relative to the vertical component, as mentioned above and this results in elliptical polarization. An observation is made on the ratio of: 1) the phase difference in degrees and 2) the amplitude difference in dB between the emerging horizontal and vertical components of a CP wave incident on the rain path. This ratio has been found to be both experimentally [24] and theoretically near constant and results in the ellipse tilt angle from (4) to be essentially constant over a moderate range of rain rates. This is evident in Fig. 2 from the nearly straight radial lines of constant tilt angle emanating from the origin. This tilt angle constancy is shown by Hendrix [20].

The near constant slope tilt angle line can be derived from the following analysis. With an incident CP wave, the emerging elliptically polarized wave has an amplitude ratio x slightly greater than unity and defined as

$$x = E_v/E_h.$$

This ratio can be given in decibels as

$$\mathrm{dB}(x) = 20\log_{10}\mathrm{x}.$$

It can be shown that if x is near unity, the following approximation holds:

$$x - 1/x \doteq 2(x-1).$$

With an approximate logarithmic formulation

$$2(x-1) \doteq 2\ln \mathrm{x}$$
$$\doteq 4.6\,052\log_{10}\mathrm{x} = 0.230\,26\ \mathrm{dB}(x)$$

so that

$$x - 1/x \doteq 0.230\,26\ \mathrm{dB}(x).$$

With these approximations the ellipse tilt angle in (4) can be rewritten

$$\theta_t \doteq 90^\circ - 0.5\tan^{-1}[2\sin\phi_\mathrm{r}/(0.230\,26\ \mathrm{dB(x)})].$$

If the phase delay ϕ_{r° in degrees is small, then the tilt angle is given approximately by

$$\theta_t \doteq 90^\circ - 0.5\tan^{-1}(0.1516\phi_{\mathrm{r}^\circ}/\mathrm{dB(x)}). \quad (6)$$

The arctangent is computed in degrees. This shows that if the ratio of $\phi_r^\circ/\mathrm{dB}(x)$ is constant over a range of rain rates, the ellipse tilt angle will also be constant. This approximation for θ_t is consistent with reported measurements that with an incident CP wave the phase difference between the emerging co-pol to cross-pol components lies substantially in the third quadrant [25]. The $\theta_t = 0^\circ$ orientation of the phase reference axis for both CP co-pol and cross-pol components is taken to be horizontal.

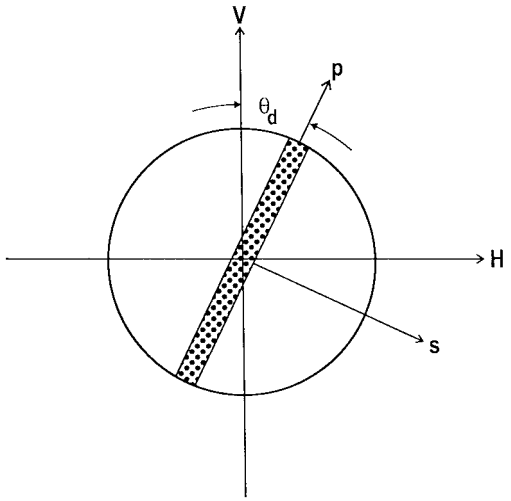

Fig. 3. Central cross section of a dielectric plate transducer in a circular waveguide. The dielectric plate is oriented at an angle of θ_d from vertical. A phase difference of ϕ_d is introduced between the principal planes of the plate. If $\theta_d = 0^\circ$, a phase delay is introduced to only the vertical component of the electric field. Impedance match is assumed.

IV. Mitigation of Cross Polarization with Fixed Phase Delay

For a system application, it is assumed that perfect cancellation of cross polarization may not be necessary and a mitigated XPD value such as 22 dB may be adequate. Two separate cases are discussed—the first with only ice particles and the second with rain.

A. Ice Particles

If the link encounters ice particles, the effect will be more differential phase [3]–[5], [10], [12], [26] than differential amplitude between V and H components as stated above. In this situation a vertical phase delay mitigation technique should be very beneficial.

The proposed method of mitigating cross-polarization effect on CP waves entails the addition of phase delay to only the vertical component of the wave emerging from the ice particle and rain path as shown in Fig. 1(b). This technique has been reported [5], [7], [8]. The wave emerges elliptically polarized with the horizontal component that is phase delayed and attenuated more relative to those of the vertical component. For mitigation, a phase delay is added to the vertical component and the signal is recovered after the OMT. This may be achieved, for example, by using a dielectric plate transducer shown in Fig. 3 with a plate angle of $\theta_d = 0^\circ$ and plate designed to provide a specific amount of phase delay. The overall performance of Fig. 1(b) is described in terms of an example. By referring to Fig. 2, if the ice particles introduce a 16° phase-delay difference with no loss difference between the horizontal and vertical components; the $\mathrm{XPD_{RHEP}}$ is about 17 dB. A phase delay as little as 9° added to the vertical component will improve the XPD significantly to about 24 dB. From OLYMPUS beacon experiments, an ice event resulted in a 27° differential phase [26] and 2-dB co-pol attenuation which corresponds to about 12-dB XPD.

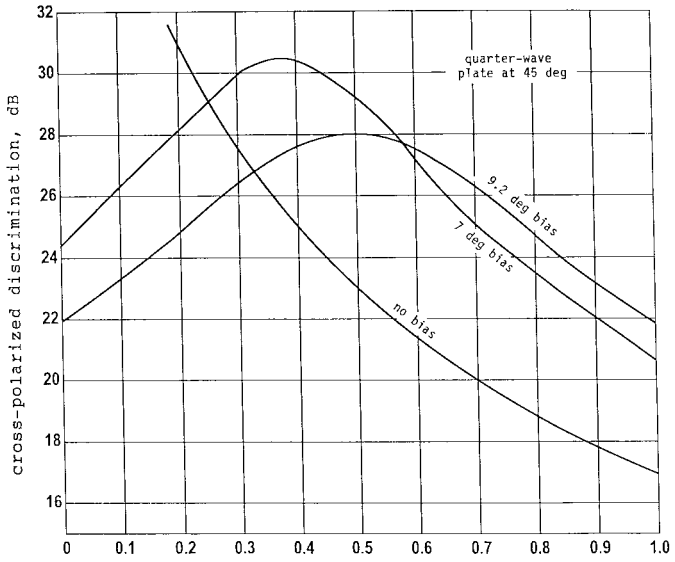

Fig. 4. Cross-polar discrimination as a function of rain path length for various values of the phase delay added to the vertical component of the received polarization.

B. Rain

For a path loss of about 9 dB due to rain (from Fang and Chen [24]), the emerging wave may have a differential amplitude of 1.2 dB and an additional phase difference of 14° between vertical and horizontal components. Without a phase compensator as in Fig. 1(a), the XPD is 17 dB, as shown by point "A" in Fig. 2; this may be unacceptable. With a vertical phase delay of 14°, as shown in Fig. 1(b) employing the dielectric plate transducer, the XPD is improved to 23 dB, as shown by point "B" in Fig. 2. Significant improvement in XPD using this technique has been suggested [5], [7], [8]. The sensitivity of XPD to ϕ_{vh} has been stressed by Allnutt [27].

The analysis was carried further to determine the performance of the vertical phase-delay technique by analytically varying the path length with the same anisotropy or varying the anisotropy for a given path length. It is noted that a fixed phase shift will degrade cross polarization in the absence of anisotropy. The results for a variable path length are shown in Fig. 4. A perfect quarter-wave plate is assumed for the OMT. In this graph, it is assumed that with different anisotropies, the ratio of 1.2-dB differential amplitude to 14° of differential phase is maintained. Three cases are described.

1) With no phase bias compensation, the XPD magnitude is 17 and 23 dB for the full and half path lengths, respectively.
2) With a 9.2° fixed phase bias ϕ_v on only the vertical component, the XPD magnitude is 21.8 dB for the two extremes of either full path length or zero length (no anisotropy) and the XPD is better for intermediate amounts of anisotropy (or path length) reaching a maximum of 28 dB for one-half the path length. This XPD behavior perhaps may be adequate for a system application.
3) In another example of 7° of ϕ_v, the XPD magnitude is 24.2 dB for zero anisotropy, a maximum of 30.5 dB near 0.4 path length and 20.7 dB for the full path length.

V. Imperfect OMT and Crossed Ellipses

By adding a fixed vertical phase bias, a significant improvement in XPD can be achieved as shown in Fig. 2; however, after the phase bias, the output wave is still elliptically polarized but with a lower axial ratio. For the 1.2 dB and 14° example, the initial emerging wave axial ratio is 2.47 dB, but with 14° of phase compensation the axial ratio can be reduced to 1.2 dB. With a residual axial ratio of 1.2 dB, it is possible to achieve perfect cancellation by employing an OMT with an axial ratio of 1.2 dB and the two polarization ellipse axes crossed at 90°. The overall coupling of crossed ellipses has been discussed by Ludwig [28] and Stutzman [16]. It is noted that an OMT with an axial ratio of 1.2 dB is actually an imperfect quarter-wave plate.

Further analysis has shown that while a particular arrangement may provide perfect cancellation of infinite XPD for one circular polarization, the XPD for the orthogonal circular polarization is a different value.

VI. Special Transducer

From an examination of the block diagram in Fig. 1(c), it is apparent that a phase bias component and a low-axial ratio transducer, which is an imperfect quarter-wave plate, can be combined into a single special transducer. This simplified circuit is illustrated in Fig. 1(d). The geometry of this dielectric plate transducer is shown in Fig. 3. The dielectric plate is oriented at an angle of θ_d from vertical and a phase difference of ϕ_d is introduced between the principal planes of the plate.

The formulation of this combined function can be derived from another paper [17]. A sample computation was performed assuming 1.2 dB and 14° differences between the vertical and horizontal components and the results are shown in Fig. 5. The abscissa is the phase differential ϕ_d of the dielectric plate and the ordinate is the plate angle θ_d from vertical. If θ_d is 45° and ϕ_d is 90°, which are parameters for an ideal OMT or quarter-wave plate, the CP depolarizations for both RHCP and LHCP are equal in magnitude at 17.03 dB. The equal XPD can be improved to 23.21 dB if $\theta_d = 38°$ and $\phi_d = 93.4°$. This is illustrated by the central group of dark circles.

If the incident wave is LHCP, perfect cancellation can be achieved with $\theta_d = 39°$ and $\phi_d = 101°$. However, for an incident RHCP, the RL/XPD is 17.1 dB (not shown) with the foregoing parameters; thus, the XPD magnitudes are not equal. With an incident RHCP the RL/XPD can be made infinite by choosing specific values of $\theta_d = 37.1°$ and $\phi_d = 86°$. For LHCP with these transducer parameters, the LR/XPD becomes poor at 17.1 dB.

VII. Conclusions

For moderate anisotropy with a 1.2-dB amplitude and 14° phase differences between vertical and horizontal components of an incident circularly polarized wave, the analysis shows that a fixed passive transducer can mitigate cross-polarization performance from an initial 17 dB to about 22 dB. This residual value of XPD may be adequate for some system applications. With less anisotropy, the XPD is better than 22 dB. Over a greater range of anisotropy, it appears possible to

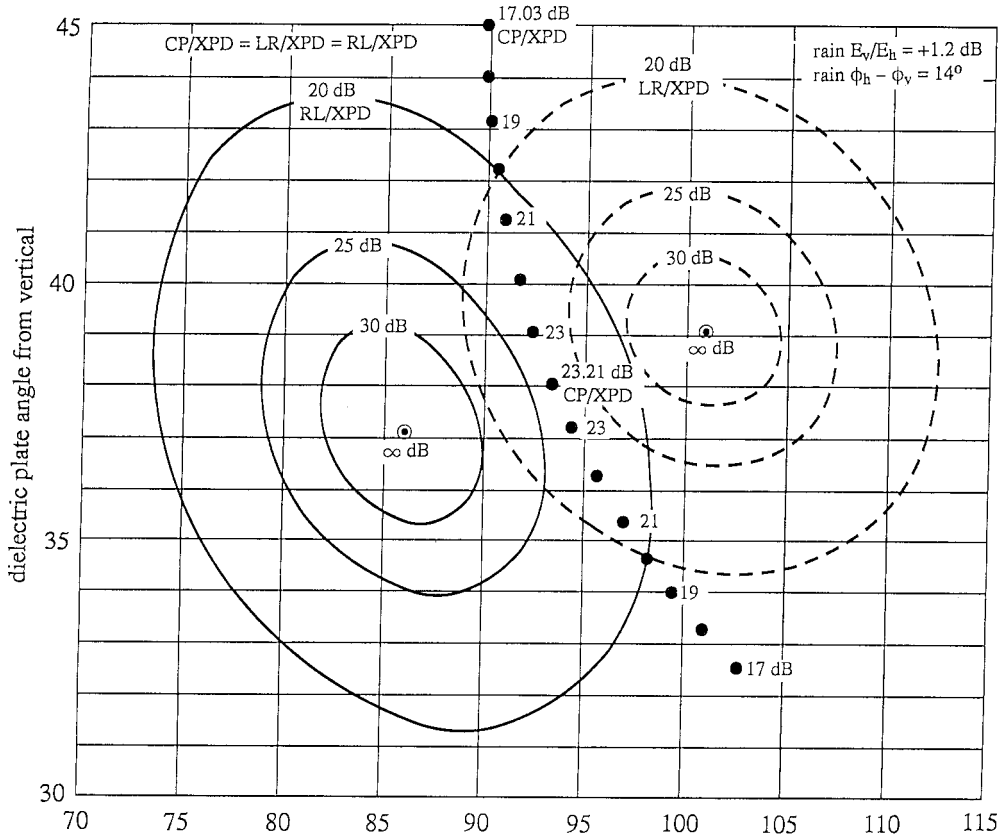

Fig. 5. Output cross-polarized discrimination of a circularly polarized wave using special transducer as a function of the parameters of the dielectric plate. Either a left or right circularly polarized wave is incident on the rain path. In this example, it is assumed that the rain causes the horizontal relative to the vertical component to emerge attenuated by 1.2 dB and phase delayed by 14°.

adjust in steps the phase delay approximately in proportion to the co-pol attenuation or loss in signal level.

For the general case with this special transducer approach, the amount of cross-polarization mitigation is not equal in magnitude between right and left hand CP signals. It is possible to achieve perfect cancellation for one CP but not the other simultaneously. Further effort on this approach is suggested to determine limits of utility.

Issues not addressed are design feasibilities of the special transducer in terms of bandwidth, impedance match, and power handling capacity. For system applications, infinite values of XPD are not necessary.

APPENDIX
CROSS-POL DISCRIMINATION OF FOUR-PORT NETWORK

A four-port network applicable to a dual circularly polarized OMT is shown in Fig. 6. The input complex signals are $\boldsymbol{E}_v$ and $\boldsymbol{E}_h$ and the transducer output complex signals are $\boldsymbol{E}_{tv}$ and $\boldsymbol{E}_{th}$. For a right-hand circularly polarized wave the amplitudes of $\boldsymbol{E}_{tv}$ and $\boldsymbol{E}_{th}$ are equal and the phase of $\boldsymbol{E}_h$ relative to that of $\boldsymbol{E}_v$ lags by 90°. However, if the circularly polarized wave encounters rain and ice particles, there is an additional phase lag of ϕ_r on the $\boldsymbol{E}_h$ component and the wave becomes elliptically polarized.

An OMT or quarter-wave plate can be designed in a circular waveguide with a dielectric plate 1) inclined at an angle of $\theta_d = 45°$ to the vertical or horizontal electric field and 2) a phase lag of $\phi_d = 90°$ for the electric field parallel to the plate relative to that for the field perpendicular to the plate. Such a conceptual transducer is depicted in Fig. 3.

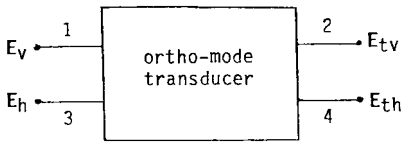

Fig. 6. Four-port network representing an OMT.

By referring to the formulation given in [17], the two signals emerging from this four-port network are given by

$$\boldsymbol{E}_{tv} = \boldsymbol{E}_v 0.5[e^{j\pi/2} + 1] + \boldsymbol{E}_h 0.5[e^{j\pi/2} + 1]$$
$$\boldsymbol{E}_{th} = \boldsymbol{E}_v 0.5[e^{j\pi/2} - 1] + \boldsymbol{E}_h 0.5[e^{j\pi/2} + 1]. \quad \text{(A.1)}$$

The function of the OMT is to decompose an incoming RHEP wave into RHCP plus LHCP signals at the output which are $\boldsymbol{E}_{tv}$ and $\boldsymbol{E}_{th}$, respectively, in Fig. 6. The magnitude of the desired XPD of the RHEP wave is given by

$$\text{XPD}_{\text{RHEP}} = \text{RHCP/LHCP} = |\boldsymbol{E}_{tv}/\boldsymbol{E}_{th}|$$

and

$$\text{XPD}_{\text{RHEP}} = \left|\frac{\boldsymbol{E}_v e^{j\pi/4} + \boldsymbol{E}_h e^{j3\pi/4}}{\boldsymbol{E}_v e^{j3\pi/4} + \boldsymbol{E}_h e^{j\pi/4}}\right|. \quad \text{(A.2)}$$

After dividing the numerator terms by $e^{j\pi/4}$ and the denominator terms by $e^{j3\pi/4}$ and noting that $\boldsymbol{E}_h = E_h e^{(-j\pi/2-\phi_r)}$ and $\boldsymbol{E}_v = E_v$

$$\mathrm{XPD_{RHEP}} = \left| \frac{E_v + E_h e^{-j\phi_r}}{E_v - E_h e^{-j\phi_r}} \right|. \tag{A.3}$$

or, in decibels

$$\mathrm{XPD_{RHEP}} = 20\log_{10}\left| \frac{\mathrm{E_v} + \mathrm{E_h e^{j\phi_r}}}{\mathrm{E_v} - \mathrm{E_h e^{j\phi_r}}} \right|. \tag{A.4}$$

ACKNOWLEDGMENT

The author would like to thank the anonymous reviewers for their numerous knowledgeable and constructive comments. He would also like to thank G. D. Gilliam for discussions about the mitigation of anisotropic cross-polarization effects on a circularly polarized wave using a fixed phase delay on the vertical polarization component. He would also like to acknowledge the comments offered by R. C. Ligmanowski and R. C. Steuer.

REFERENCES

[1] H. B. Poza, "TDRSS telecommunication payload: An overview," *IEEE Trans. Aerosp. Elect. Syst.*, vol. AES-15, pp. 414–429, May 1979.
[2] T. Oguchi, "Electromagnetic wave propagation and scattering in rain and other hydrometeors," *Proc. IEEE*, vol. 71, pp. 1029–1078, Sept. 1983.
[3] H. W. Arnold, D. C. Cox, H. H. Hoffman, and R. P. Leck, "Characteristics of rain and ice depolarization for a 19- and 28-GHz propagation path from a Comstar satellite," *IEEE Trans. Antennas Propagat.*, vol. AP-28, pp. 22–28, Jan. 1980.
[4] R. A. Hogers, M. H. A. J. Herben, and G. Brussaard, "Distinction between rain and ice depolarization by calculation of differential attenuation and phase shift," *Electron. Lett.*, vol. 27, no. 19, pp. 1752–1753, Sept. 1991.
[5] Y. Maekawa, N. S. Chang, A. Miyazaki, and T. Segawa, "Calculation of depolarization cancellation on Ka-band satellite-to-ground paths," in *Dig. IEEE Int. Antennas Propagat. Symp.*, Seattle, WA, 1991, pp. 1560–1563.
[6] F. Dintelmann, G. Ortgies, F. Rücker, and R. Jakoby, "Results from 12- to 30-GHz German experiments carried out with radiometers and the OLYMPUS satellite," *Proc. IEEE*, vol. 81, pp. 876–884, June 1993.
[7] Y. Maekawa, N. S. Chang, and A. Miyazaki, "Cross-polarization discrimination measurements on satellite-to-ground path using CS-3 beacon signal," *Dig. Int. Geosci. Remote Sensing Symp.*, 1993, vol. 1, pp. 295–297.
[8] R. Jakoby and R. Rücker, "Crosstalk cancellation on satellite links in the K_a band," *Dig. IEEE Int. Antennas Propagat. Symp.*, Seattle, WA, 1994, pp. 1328–1331.
[9] R. Jakoby, F. Rücker, D. Vanhoenacker, and H. Vasseur, "Fraction of ice depolarization on satellite links in Ka band," *Electron. Lett.*, vol. 30, no. 23, pp. 1917–1918, Nov. 1994.
[10] R. Jakoby, "Results of 20/12.5 and 30/20-GHz XPD-frequency scaling measurements with the Olympus satellite," *IEEE Trans. Antennas Propagat.*, vol. 43, pp. 1503–1508, Dec. 1995.
[11] Y. Karasawa and Y. Maekawa, "Ka-band earth-space propagation research in Japan," *Proc. IEEE*, vol. 85, pp. 821–842, June 1997.
[12] B. R. Arbesser-Rastburg and A. Paraboni, "European research on Ka-band slant-path propagation," *Proc. IEEE*, vol. 85, pp. 843–852, June 1997.
[13] I. J. Caylor and V. Chandrasekhar, "Time-varying ice crystal orientation in thunderstorms observed with multiparameter radar," *IEEE Trans. Geosci. Remote Sensing*, vol. 34, pp. 847–858, July 1996.
[14] R. W. Kreutel, Jr., D. F. DiFonzo, W. J. English, and R. W. Gruner, "Antenna technology for frequency reuse satellite communications," *Proc. IEEE*, vol. 65, pp. 370–378, Mar. 1977.
[15] M. Yamada, H. Yuki, and K. Inagaki, "Compensation techniques for rain depolarization in satellite communications," *Radio Sci.*, vol. 17, pp. 1220–1230, Sept./Oct. 1982.
[16] W. L. Stutzman, *Polarization in Electromagnetic Systems.* Boston: Artech House, 1993.
[17] K. Tomiyasu, "Four-port scattering matrix for dual-polarized wave transmission and reflection network," *IEEE Trans. Microwave Theory Tech.*, vol. 45, pp. 354–358, Mar. 1997.
[18] J. D. Kraus, *Radio Astronomy.* New York: McGraw-Hill, 1966.
[19] M. Born and E. Wolf, *Principles of Optics*, 6th ed. New York: Pergamon Press, 1993.
[20] C. E. Hendrix, G. Kulon, and T. A. Russell, "Specification of polarization parameters for optical-performance in rain of dual circularly polarized radio links," *IEEE Trans. Antennas Propagat.*, vol. 40, pp. 510–516, May 1992.
[21] C. Balanis, *Advanced Engineering Electromagnetics.* New York: Wiley, 1989.
[22] C. Balanis, *Antenna Theory, Analysis, and Design*, 2nd ed. New York: Wiley, 1997.
[23] C. Capsoni, A. Paraboni, F. Fedi, and D. Maggiori, "A model-oriented approach to measure rain-induced cross-polarization," *Ann. Telecommun.*, vol. 36, pp. 154–159, Jan./Feb. 1981.
[24] D. J. Fang and C. H. Chen, "Propagation of centimeter/millimeter waves along a slant path through precipitation," *Radio Sci.*, vol. 17, pp. 989–1005, Sept./Oct. 1982.
[25] H. Fukuchi, J. Awaka, and T. Oguchi, "A theoretical formula for the prediction of cross-polarized signal phase," *IEEE Trans. Antennas Propagat.*, vol. 33, pp. 997–1002, Sept. 1985.
[26] G. Brussaard, "The analysis of depolarization and anisotropy using the OLYMPUS beacon," in *Proc. Olympus Utilization Conf.*, Seville, Spain, Apr. 1993, pp. 561–565.
[27] J. E. Allnutt, *Satellite-to-Ground Radiowave Propagation.* London, U.K.: Peter Peregrinus, 1989.
[28] A. C. Ludwig, "A simple graph for determining polarization loss," *Microwave J.*, vol. 19, p. 63, Sept. 1976.

Kiyo Tomiyasu (S'41–A'42–M'49–SM'52–F'62–LF'85) was born in Las Vegas, NV, on September 25, 1919. He received the B.S. degree in electrical engineering from the California Institute of Technology, Pasadena, in 1940, the M.S. degree in communication engineering from Columbia University, New York, NY, in 1941, and the Ph.D. degree in engineering science and applied physics from Harvard University, Cambridge, MA, in 1948.

In 1949, he joined the Sperry Gyroscope Company, Great Neck, NY, as a Project Engineer. In 1955 he joined the General Electric Microwave Laboratory, Palo Alto, CA, as a Consulting Engineer, and five years later he transferred to the General Electric Research and Development Center, Schenectady, NY, where he was involved with lasers and microwave projects. In 1969 he became a Consulting Engineer at the General Electric Valley Forge Space Center, Philadelphia, PA. For several years he has been involved with microwave remote sensing of the earth using satellite-borne radiometers, scatterometers, and synthetic aperture radars. As a result of corporate mergers in 1995, he is now employed by Lockheed Martin Corporation, Philadelphia, PA, and is an M&DS Fellow.

Dr. Tomiyasu was President of the IEEE Microwave Theory and Techniques Society during 1960–1961, and subsequently served on its Nominations Committee and Awards Committee. He was the Editor of that Society's TRANSACTIONS in 1958 and 1959 and Guest Editor of the May 1978 Special Issue on High Power Microwaves. In 1973 he was elected Honorary Life Member of the Society and its Administrative Committee. He was named recipient of the Microwave Career Award in 1980 and the Distinguished Service Award in 1987 and was the recipient of an IEEE Centennial Medal in 1984. He is currently a member of the Administrative Committee of the IEEE Geoscience and Remote Sensing Society, and he received its Outstanding Service Award in 1986. He has served on the IEEE Publications Board, the Technical Activities Board, the Awards Board, the Board of Directors and the Educational Activities Board. His name is listed in several biographical references, among which are *American Men and Women of Science*, *Who's Who in Engineering*, *Men of Achievement*, *Leaders in Electronics*, and *Who's Who in America*. He is also a member of the American Physical Society.